Research Article J. Electrochem. Sci. Technol., 2019, 10(2), 170-176

Redox-Active Self-Assembled Monolayer on Au ultramicroelectrode and its Electrocatalytic Detection of *p*-aminophenol Oxidation

Yun Jee Kim†, Ki Jun Kim†, Seung Yeon Jung, You Jin Hwang, and Seong Jung Kwon*
Department of Chemistry, Konkuk University, 120 Neungdong-ro, Gwangjin-gu, Seoul 05029, Korea

ABSTRACT

Alkanethiol self-assembled monolayers (SAMs) and partially ferrocene (Fc) modifications were applied to the Au ultramicroelectrode (UME) rather than to standard sized electrodes with dimension of millimeters. The electron transfer mediation of the SAMs and Fc modified Au UME was investigated by using a *p*-aminophenol (*p*-AP) oxidation reaction via cyclic voltammetry. The electrocatalytic *p*-AP oxidation at the SAMs and Fc modified Au UME showed a much larger electrocatalytic current density than that at the standard sized electrode due to the fast mass transfer rate at the UME.

Keywords : Self-assembled monolayers, Ferrocene, Ultramicroelectrode, Electrocatalytic reaction, *p*-aminophenol, Redox-active

Received : 21 September 2018, Accepted : 10 November 2018

1. Introduction

Self-assembled monolayers (SAMs) can provide a reproducible and robust route to functionalize electrode surfaces by using organic molecules containing anchor groups such as thiols, amines, or silanes [1-5]. The SAMs allow tremendous flexibility for several applications depending on their terminal functional group and chain length. For example, thiol-linked SAMs are widely used to immobilize biomolecules on the Au electrode surfaces, because they provide a cell membrane-like microenvironment that contains a variety of functional groups that are useful for efficient covalent immobilization of biological molecules [6-8].

The surface of SAMs-modified electrodes is important in electrochemical biosensors because the additional organic layers of SAMs and biomolecules make the electron transfer difficult, ultimately leading to the blockage of direct electron transfer of electroactive species into the electrode [9,10]. Therefore, redox-mediating functional groups that enable electron transfer between electroactive species and the SAMs-modified electrodes are required for electrochemical detection with such electrodes. A variety of redox species including transition metal complexes (e.g., ferrocene (Fc) [11,12], Ru complexes [13,14], and Os complexes [15]) and organic molecules (e.g., methylene blue [16]) are attracting interest as the electron-transfer mediator of SAMs-modified electrodes. The mediator-introduced redox-active SAMs can provide an excellent platform that helps exploit electrochemistry for biosensors.

The Fc-modified SAMs are one of the most widely used redox-active SAMs. The Kwak group introduced a partially ferrocenyl-tethered dendrimer (Fc-D) to solve the electrons transfer problem in the SAMs modified electrodes [17-19]. Fc in Fc-D acts as a redox mediator and its dendrimer develops a pathway for the electron transfer [20]; therefore, Fc-D modified SAMs show outstanding redox mediation for the oxidation of alkaline phosphatase (ALP)-generated *p*-aminophenol (*p*-AP). The combination of ALP and *p*-AP is widely used as an enzyme and as a signal-reporting molecule in electrochemical biosensors using enzyme labeling [21-23].

The electron-transfer mediation of *p*-AP oxidation by Fc is regarded as an electrochemical catalytic (EC′) reaction. Therefore, the mass transfer rate of *p*-AP to the electrode surface affects the electrocatalytic

†These authors contributed equally.
*E-mail address: sjkwon@konkuk.ac.kr

DOI: https://doi.org/10.5229/JECST.2019.10.2.170

current by the EC′ reaction. The mass transfer rate at the ultramicroelectrode (UME) is faster than that obtained with the standard sized electrode [24], which, depending on its application, might have dimensions of meters, centimeters, or millimeters. Therefore, if the redox-active SAMs are introduced on the UME rather than on the standard sized electrode, a high electrocatalytic current with respect to electrode area by electron-transfer mediation is expected owing to the fast mass transfer rate of electroactive species. Some other advantages of SAMs-modified UME are the reusability of the UME by polishing and its low background current owing to its comparatively small size; these features of such UMEs are particularly useful when they are used as a platform for electrochemical biosensors. Despite such advantages, the UME has not been used as a substrate for SAMs owing to the high cost and difficult accessibility compared with the standard sized electrode.

Therefore, in this paper, we introduce SAMs and Fc modification on an Au UME and investigate the electron transfer mediation of redox-active SAMs on the UME. The electrocatalytic current produced by *p*-AP oxidation at SAMs and Fc modified Au UME was measured via cyclic voltammetry (CV), and the results are compared with that obtained at millimeter-sized Au electrode modified with the same SAMs and Fc.

2. Experimental

2.1 Reagents

Amine-terminated G4 poly(amidoamine) (PAMAM) dendrimer, ferrocenecarboxaldehyde, 11-ferrocenyl-1-undecanethiol (11-Fc-thiol), 1-ethyl-3-[3-(dimethylamino)propyl]carbodiimide hydrochloride (EDC), N-hydroxysuccinimde (NHS), sodium borohydride, *p*-AP, 12-mercaptododecanoic acid (MDA), and 11-mercapto-1-undecanol (MUO) were purchased from Sigma-Aldrich. All buffer salts and other inorganic chemicals were also obtained from Sigma-Aldrich. The rinsing buffer comprised 50 mM tris(hydroxymethyl)aminomethane hydrochloride (Tris), 0.5 M NaCl, and 0.05 %(v/v) Tween 20 (pH 7.4). The electrolyte solution for the electrochemical experiment consisted of 50 mM Tris, 10 mM KCl, and 1 g/L $MgCl_2$ (pH 9.0) with/without *p*-AP. Ultrapure water (> 18 MΩ, Millipore) was used in all experiments.

2.2 Preparation of Fc-D

The Fc-D was synthesized by an imine formation reaction between the partial primary amines of G4 PAMAM dendrimers and ferrocenecarboxaldehyde following the reported procedure [25,26]. In brief, ferrocenecarboxaldehyde (4.5 mg) was dissolved in 2 mL of methanol, and the mixture was added dropwise to 0.15 mL of 10 % (w/w) G4 PAMAM dendrimer solution containing hydrochloric acid as a catalyst. The reaction mixture was slowly stirred for 2 h. A solution of sodium borohydride (3 mg in 2 mL methanol) was slowly added, and the resulting solution was stirred for 1 h to reduce carbon-to-nitrogen double bonds. The reaction product was purified by lipophilic gel permeation chromatography (Sephadex LH-20, GE Healthcare Bio-Sciences AB) using methanol as the eluent.

2.3 Preparation of Au electrode and UME

Au electrodes were prepared by electron beam evaporation of 40 nm of Ti and 150 nm Au onto Si (100) wafers. Au UMEs were prepared by using the following method. [27] In brief, a Au (10 μm diameter) wire was sealed in glass, after rinsing with water. The Au wire was connected to a Cu lead with silver epoxy, and the electrode was polished with a suspension of alumina powder in water until a mirror face was achieved. The diameter of the Au electrode was 4.5 mm and that of the Au UME was 10 μm. Both electrodes are 2D disk type.

2.4 SAMs and Fc modification on Au electrode or UME

SAMs and Fc-D modification on the electrodes was prepared as shown in Scheme 1. Au electrode or UME were cleaned in piranha solution (H_2O_2 : H_2SO_4 (v/v) = 1:3), rinsed with water, and then dried with nitrogen gas. The clean electrodes were immersed in a mixed methanol solution of MDA and MUO (1 mM and 4 mM, respectively) for 18 h, washed with pure methanol, and dried with nitrogen gas. The optimized incubating time for SAMs formation on the UME was 18 h. When the incubating time was <12 h, the electrode showed erratic Fc oxidation current, indicating irreproducible SAMs, after Fc-D modification step. Then, the carboxylic groups of MDA were activated by immersing the electrodes into a mixed aqueous solution of 50 mM EDC and 25 mM NHS for 3 h. Next, the Au electrode and UME were incubated in the Fc-D stock solution (100 μL) for 2 h either by spotted or immersed. The

electrostatically attached Fc-D was removed by rinsing the electrode with rinsing buffer.

The other Fc modified Au electrodes (11-Fc-thiol mixed SAMs modified electrode) were prepared by immersing the clean electrode in mixtures of 11-Fc-thiol and MUO for 18 h. The mole fraction of 11-Fc-thiol and MUO in the methanol solution was 1:9 (0.1 mM and 0.9 mM, respectively). The incubated electrodes were washed with pure methanol and dried under nitrogen gas.

2.5 Electrochemical cell and instrumentation

The electrochemical experiment was performed using a CHI model 660 potentiostat (CH Instruments, Austin, TX) with the three electrode cell placed in a Faraday cage. The electrochemical cell comprised a SAMs modified working electrode, a Pt wire counter-electrode, and an Ag/AgCl reference electrode or mercury-mercuric sulfate reference electrode. The electrolyte solution with *p*-AP was prepared daily.

3. Results and Discussion

To characterize the immobilization of the Fc moiety onto the SAMs modified electrodes, the redox reaction of Fc was investigated by CV. Two different Fc moiety modified electrodes were prepared. One is a SAMs and Fc-D modified electrode and the other is

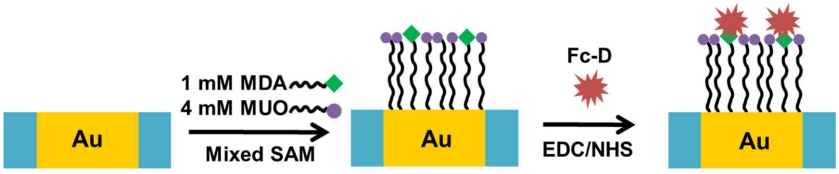

Scheme 1. Schematic illustration of the formation of mixed SAMs and immobilization of Fc-D on Au electrodes.

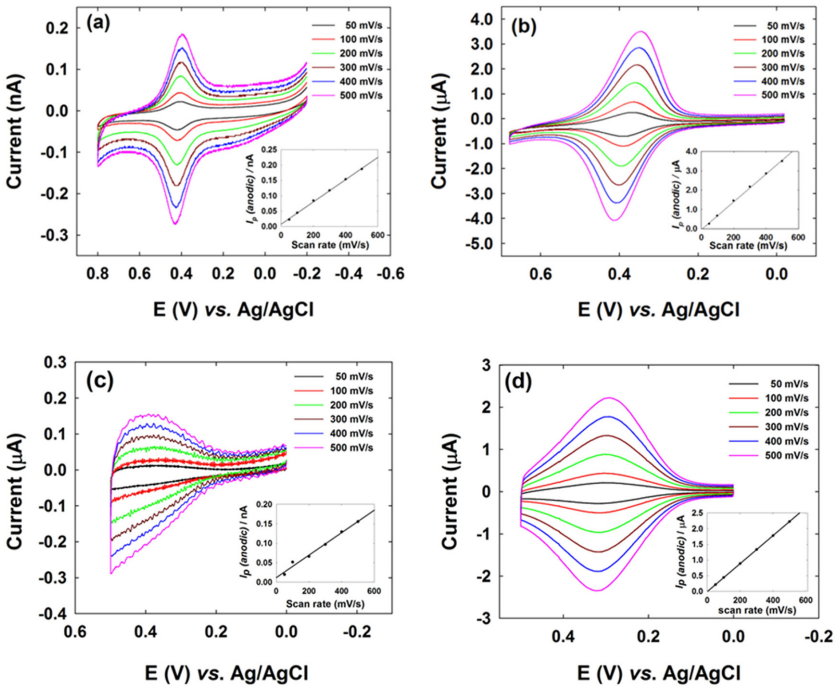

Fig. 1. Cyclic voltammograms of (a) SAMs and Fc-D-modified Au UME (10 μm diameter) or (b) Au electrode (4.5 mm diameter) and (c) 11-Fc-thiol mixed SAMs modified Au UME (10 μm diameter) or (d) Au electrode (4.5 mm diameter), by varying the scan rate from 50 to 500 mV/s in electrolyte solution. (Inset box) Plot of anodic peak currents vs. potential sweep rates.

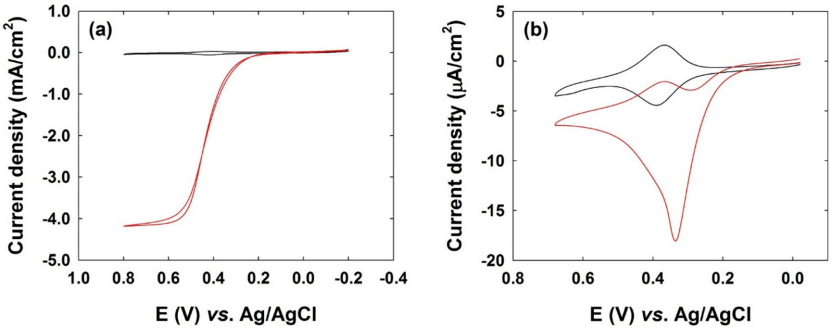

Fig. 2. Cyclic voltammograms of (a) Fc-D modified Au UME and (b) Fc-D modified Au electrode in electrolyte solution with (red)/without (black) 0.5 mM *p*-AP. Scan rate was 50 mV/s.

a 11-Fc-thiol mixed SAMs modified electrode. Fig. 1 shows cyclic voltammograms of the Fc modified Au UMEs or Au electrodes in electrolyte solution. As shown in Fig. 1, the peak currents increase linearly with the scan rate. The full width at half-maximums (FWHM) were ~110 mV (105 and 120 mV at Fig. 1a and 1b, respectively) at the SAMs and Fc-D modified electrodes and ~210 mV (~200 and 218 mV at Fig. 1c and 1d, respectively) at the 11-Fc-thiol mixed SAMs modified electrodes. The FWHM value of the SAMs and Fc-D modified electrodes, ~ 110 mV, approximately indicates the ideal value for reversible responses, 90.6/n mV, where the number of electron transfer, *n*, is 1 for the Fc oxidation [17]. Therefore, the SAMs and Fc-D modified electrode show better typical CV features of the surface-bound species than the 11-Fc-thiol mixed SAMs modified electrode. In addition, the reproducibility of the peak was also better in the SAMs and Fc-D modified electrode than the 11-Fc-thiol mixed SAMs modified electrode. Considering these, the SAMs and Fc-D modification seems a more effective way to introduce the Fc-moiety on the Au UME than the modification using 11-Fc-thiol. Therefore, we used the SAMs and Fc-D modification to introduce Fc moiety on the UME for the later experiment.

From the cyclic voltammogram, the surface coverage of the Fc moiety on the SAMs was calculated from the coulometric charge by integrating the anodic peak area in the CVs of Fig. 1, assuming that all the Fc sites are electrochemically active [28]. Using this approach, the calculated average values (±standard deviation) of surface concentration of Fc, Γ_s, were $4.9(\pm1.5)\times10^{-10}$ and $2.2(\pm0.12)\times10^{-10}$ mol/cm^2 at the SAMs and Fc-D modified Au UME and Au electrode, respectively.

As calculated above, the surface coverage by Fc sites had almost the same order of magnitude at both the Au UME and Au electrode. Moreover, the redox potential for the Fc redox reaction at each electrode was also identical. This indicates that the formation of SAMs on the Au UME was as successful as that on the Au electrode. Even though the reproducibility of SAM modification on the UME was a little lower than that at the Au electrode, as shown as the large standard deviation, there is no big difference in the quality of the SAM on both electrodes.

To characterize the electrocatalytic performance of the Fc-D layer, the SAMs and Fc-D-modified Au UME and Au electrode were investigated by CV in electrolyte solution containing 0.5 mM *p*-AP. As shown in Fig. 2, in the presence of *p*-AP, the oxidation part at both the UME and standard sized electrode were amplified by the electrocatalytic redox-mediated oxidation of *p*-AP, even though the reduction part stayed intact. First, the Fc moiety on SAMs is oxidized to the ferrocenium ion (Fc^+) by the electrochemical oxidation reaction. Then, the Fc^+ is reduced back to Fc by the chemical redox reaction with *p*-AP. As discussed in a previous report, this can be explained by the following mechanism [17,18],

$$2Fc \rightarrow 2Fc^+ + 2e^- \quad (1)$$

$$2Fc^+ + p-AP \xrightarrow{k'} quinoimide + 2Fc + 2H^+ \quad (2)$$

where quinoimide (QI) is a molecule of *p*-AP that has been oxidized by the loss of two electrons. When the

potential scan is reversed, none or a small cathodic current was observed, corresponding to the reduction of QI or electron transfer from Fc to QI.

Depending on the size of electrode, the peak-shape appearance was obtained with the Au electrode, and the steady-state current was obtained with the Au UME. However, the shape of CV can be changed as a function of kinetic parameter, λ; [24]

$$\lambda = \frac{k' C_{AP}^{*}}{\nu}\left(\frac{RT}{nF}\right) \quad (3)$$

where k' is the kinetic constant of the second reaction step, C_{AP}^{*} is the initial concentration of *p*-AP, and ν is the scan rate. When λ becomes large, the i-E curve loses its peak-shaped appearance and becomes a wave. Therefore, the limiting current is experimentally obtainable even in the standard sized electrode when the scan rate is slow. However, in the case of the Au UME, the limiting current is easily obtained even in a fast scan rate condition. This is owing to the fast mass transfer rate at the UME than the standard sized electrode.

In addition, the electrocatalytic current amplification ratio with/without *p*-AP was ~8.4 times higher at the UME than at the standard sized electrode. This huge enhancement also occurred because of the fast mass transfer rate at the UME.

Cyclic voltammograms of the SAMs and Fc-D-modified Au UME and Au electrode were obtained in an electrolyte solution containing various concentrations of *p*-AP as shown in Fig. 3. Due to the fast mass transfer in the UME, the limiting current by the

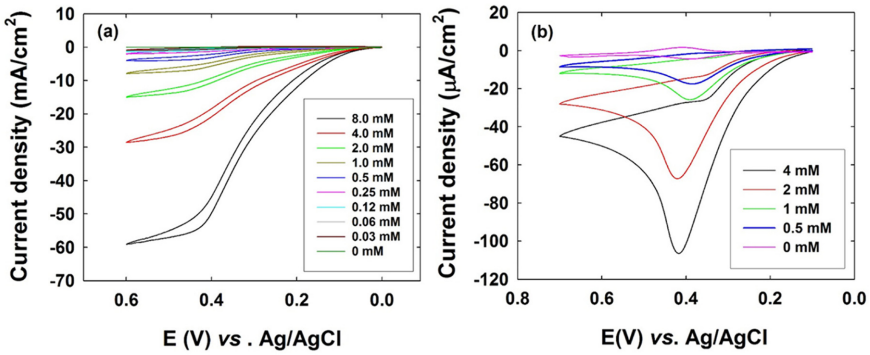

Fig. 3. Cyclic voltammograms of (a) Fc-D modified Au UME and (b) Fc-D modified Au electrode in electrolyte solution containing various concentrations of *p*-AP. Scan rate was 50 mV/s.

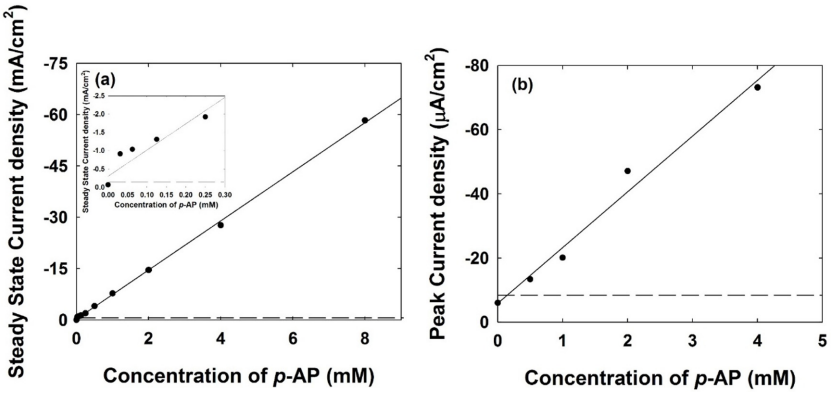

Fig. 4. Calibration plot corresponding to change (a) in anodic limiting current for Fc-D modified Au UME and (b) in anodic peak current for Fc-D modified Au electrode upon different concentration of *p*-AP. The detecting limit (dashed line) was determined by multiplying the standard deviation of zero concentration results by 3.

surface bounded electrocatalyst was obtained in the Fc-D-modified Au UME. The both limiting current for UME and peak current for standard sized electrode increased in proportion to the concentrations of *p*-AP, as shown in Fig. 4.

When the electrochemical reaction (step (1)) is faster than the chemical reaction (step (2)), in this case, the second step became the rate-determining step and the limiting current can be expressed as below: [24]

$$i_{lim} = 4nFADC_{AP}r \quad (4)$$

where the D is diffusion coefficient of *p*-AP. Interestingly, the limiting current is independent to the Γ_s, when the kinetics of step (1) is much faster than step (2) and the initial concentration of *p*-AP is big enough comparing with Γ_s. Also, the limiting current is independent on the scan rate at the UME, as shown in the Fig. 5.

If the reaction condition differs with the condition above, the heterogeneous electrocatalytic current is obtained as below: [29,30]

$$i_{cat} \propto \frac{nFA\Gamma_s k' C_{AP}}{C_{AP} + K_M} \quad (5)$$

where the K_M is Michaelis constant.

The anodic steady-state current and peak currents in the cyclic voltammograms were plotted to determine the detection limit for *p*-AP (Fig. 4). The calculated detection limit for *p*-AP was 0.03 mM at Fc-D-modified Au UME and 0.5 mM for Fc-D-modified Au electrode, respectively. One order of lower detection limit was obtained at Fc-D-modified Au UME. This indicated that more sensitive detection of *p*-AP is possible using the Fc-D-modified Au UME.

As mentioned introduction, the ALP generates the electroactive species *p*-AP from its substrate *p*-aminophenyl phosphate (*p*-APP). Therefore, this approach can be used in an electrochemical biosensor employing enzyme labelling methods such as an enzyme-linked immunosorbent assay [21] in which the enzymatic properties of ALP cause amplification, affording a higher sensitivity to the method. Therefore, the electrocatalytic detection of *p*-AP can be broadened to any biosensor using the ALP enzyme label. Hence, the use of the UME as a supporting electrode to introduce redox-active SAMs is more promising in the application of biosensor platforms than the standard sized electrode.

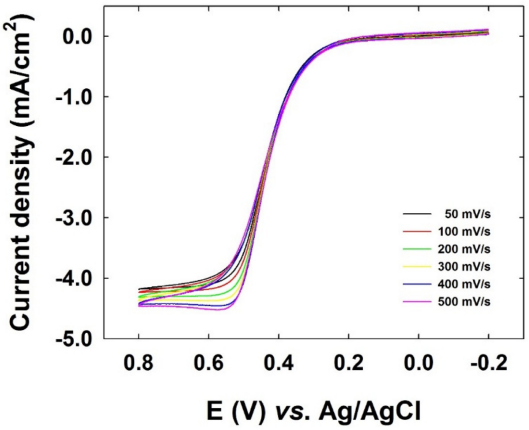

Fig. 5. Cyclic voltammogram of SAMs and Fc-D modified Au UME in electrolyte solution containing 0.5 mM of *p*-AP by varying the scan rate from 50 to 500 mV/s.

4. Conclusions

We introduced SAMs and Fc moiety onto the Au UME, which can be applied to highly sensitive electrocatalytic sensing platforms for biosensors. The electron-transfer mediation of the SAMs and Fc-D–modified Au UME was measured by using *p*-AP oxidation reaction. The limiting current is easily obtained even in a fast scan rate condition, where the peak shape appears in standard sized electrodes. The electrocatalytic current amplification ratio with/without *p*-AP at Au UME was ~8.4 times higher than that achieved with the Au electrode. In addition, the detection limit of *p*-AP concentration was one order of magnitude lower at the Au UME. Therefore, the redox-active SAM on the UME is more advantageous in many applications compared to the SAM on the standard sized electrode.

Acknowledgement

This work was supported by Konkuk University in 2016.

References

[1] L.H. Dubois and R.G. Nuzzo, *Annu. Rev. Phys. Chem.*, **1992**, *43(1)*, 437-463.

[2] A. Ulman, *An Introduction to Ultrathin Organic Films: From Langmuir-Blogett to Self-Assembly.*, Academic

Press Inc, New York. **1991**.
[3] D. Mandler and I. Turyan, *Electroanalysis*, **1996**, *8(3)*, 207-213.
[4] P.E. Laibinis and G.M. Whitesides, *J. Am. Chem. Soc*., **1992**, *114(23)*, 9022-9028.
[5] F. Patolsky, A. Lichtenstein and I. Willner, *Nat. Biotechnol.,* **2001**, *19*, 247-253.
[6] T. Wink, S. J. van Zuilen, A. Bult and W. P. van Bennekom, *Analyst*, **1997**, *122(4)*, 43R-50R.
[7] N.K. Chaki and K. Vijayamohanan, *Biosen. Bioelectron.,* **2002**, *17(1-2)*, 1-12.
[8] J.J. Gooding and D.B. Hibbert, *Trends Analyt. Chem.*, **1999**, *18(8)*, 525-533.
[9] A.L. Eckermann, D.J. Feld, J.A. Shaw and T.J. Meade, *Coord. Chem. Rev.*, **2010**, *254(15-16)*, 1769-1802.
[10] M.E.G. Lyons, *Sensors*, **2003**, *3(2)*, 19-42.
[11] S.J. Kwon, N. Park, D. Kwon and J. Kwak, *J. Nanosci. Nanotechnol*., **2011**, *11(5)*, 4194-4199.
[12] K. Uosaki, Y. Sato and H.Kita, *Electrochim. Acta*, **1991**, *36(11–12)*, 1799-1801.
[13] B. Liu, A.J. Bard, M.V. Mirkin and S.E. Creager, *J. Am. Chem. Soc.*, **2004**, *126(5)*, 1485-1492.
[14] J.F. Smalley, H.O. Finklea, C.E.D. Chidsey, M.R. Linford, S.E. Creager, J.P. Ferraris, K. Chalfant, T. Zawodzinsk , S.W. Feldberg and M.D. Newton, J. *Am. Chem. Soc.*, **2003**, *125(7)*, 2004-2013.
[15] M.E. Napier, C.R. Loomis, M.F. Sistare, J. Kim, A.E. Ecrkhardt and H.H. Thorp, *Bioconjug. Chem.*, **1997**, *8(6)*, 906-913.
[16] S.E. Salamifar, M.A. Mehrgardi, S.H. Kazemi and M.F. Mousavi, *Electrochim. Acta*, **2010**, *56(2)*, 896-904.
[17] E. Kim, K. Kim, H. Yang, Y. T. Kim and J. Kwak, *Anal. Chem.*, **2003**, *75(21)*, 5665- 5672.
[18] S.J. Kwon, E. Kim, H. Yang and J. Kwak, *Analyst*, **2006**, *131(3)*, 402-406.
[19] S. J. Kwon, H. Yang, K. Jo and J. Kwak, *Analyst*, **2008**, *133(11)*, 1599-1604.
[20] S-K. Oh, L.A. Baker and R.M. Crooks, *Langmuir*, **2002**, *18(18)*, 6981-6987.
[21] R.Q. Thompson, G.C. Barone III, H.B. Halsall and W.R. Heineman, *Anal. Biochem.*, **1991**, *192(1)*, 90-95.
[22] I. Rosen and J. Rishpon, *J. Electroanal. Chem.*, **1989**, *258(1)*, 27-39.
[23] H.T. Tang, C.E. Lunte, H.B. Halsall and W.R. Heineman, *Anal. Chim. Acta*, **1988**, *214*, 187-195.
[24] A.J. Bard and L.R. Faulkner, *Electrochemical Methods, Fundamentals and Applications, 2nd ed*., John Wiley & Sons: New York, **2001**.
[25] H.C. Yoon, M-Y. Hong and H-S. Kim, *Anal. Chem.*, **2000**, *72(18)*, 4420-4427.
[26] H.C. Yoon, H. M-Y. Hong and H-S. Kim, *Anal. Biochem.*, **2000**, *282(1)*, 121-128.
[27] A.J. Bard and M.V. Mirkin, *Scanning Electrochemical Microscopy, Eds*., Marcel Dekker: New York, **2001**.
[28] K. Takada, D.J. Diaz, H.D. Abruña, I. Cuadrado, C. Casado, B. Alonso, M. Morán and J. Losada, *J. Am. Chem. Soc.*, **1997**, *119(44)*, 10763-10773.
[29] A.J. Sathrum and C.P. Kubiak, *J. Phys. Chem. Lett*., **2011**, *2(18)*, 2372-2379.
[30] A. Sucheta, R. Cammack, J. Weiner and F.A. Armstrong, *Biochemistry*, **1993**, *32(20)*, 5455-5465.